Articles in PresS. Am J Physiol Gastrointest Liver Physiol (December 20, 2007). doi:10.1152/ajpgi.00281.2007

TITLE PAGE

Differential regulation of ERK1/2 and p38 MAP kinases in VacA-induced apoptosis of gastric epithelial cells

Mi-Ran Ki[1], Hye-Rim Lee[1], Moon-Jung Goo[1], Il-Hwa Hong[1], Sun-Hee Do[1], Da-Hee Jeong[1], Hai-Jie Yang[1], Dong-Wei Yuan[1], Jin-Kyu Park[1], and Kyu-Shik Jeong[1,*]

[1]*Department of Pathology, College of Veterinary Medicine, Kyungpook National University, 702-701, Daegu, Republic of Korea*

Running title: VacA-induced SOD-1 and villin expression

[*] Address for reprints and correspondence:

Department of Pathology, College of Veterinary Medicine, Kyungpook National University, 702-701, #1370 Sangyeok-dong, Buk-ku, Daegu City, Republic of Korea

Phone: +82-53-950-5975, Fax: +82-53-950-5955, E-mail: jeongks@knu.ac.kr

ABSTRACT

Helicobacter pylori vacuolating cytotoxin A (VacA) has been considered as an apoptosis-inducing factor. Here, we investigated the mechanism of VacA-induced apoptosis in relation to the defense mechanism and MAP kinases pathway in gastric epithelial cells. AGS cells exposed to enriched VacA extracts affected the level of SOD-1 and villin. We further investigated the role of VacA in those inductions using a functional recombinant VacA (rVacA). Activation of p38 MAPK and Bax dimerization by rVacA were increased in a dose-dependent manner. rVacA-induced ERK1/2 MAPK activation was maximal at 30 min and 4 h and 1 to 4 μg/ml of rVacA. rVacA-induced SOD-1 expression was considerably diminished by inhibiting ERK1/2 MAPK and it was slightly increased by inhibiting p38 MAPK. rVacA increased or decreased villin expression depending on dose and exposure time and its expression was mainly appeared in contractile actin ring of the dividing cells. Despite cytoprotective effect, SB203580, a p38 inhibitor was unlikely to reduce VacA-induced Bax dimerization, and rather inhibited villin and Bcl2 expression, indicating that p38 may also play a role in cell proliferation or differentiation for survival after VacA intoxication. Furthermore, p38 inhibitor accelerated rVacA-induced cell death after exposure of AGS cells to H_2O_2 but ERK1/2 inhibitor protected cells from H_2O_2 insult. These results suggest that SOD-1 and villin are expressed differentially upon VacA insult depending on dose and exposure time via ERK and p38 MAP kinases; decrease in SOD-1 and villin expression coupled with Bax dimerization leads to apoptosis of gastric epithelial cells.

Key words: *Helicobacter pylori*; VacA; SOD-1; Villin; MAP kinase signaling

INTRODUCTION

Vacuolating cytotoxin (VacA), a product of vacA s1/cagA-positive *H. pylori* strains, induces large cytoplasmic vacuoles in epithelial cells with structural and functional changes, leading to apoptosis that is, in part, responsible for *H. pylori*–induced epithelial cell damage (13, 31, 48). Purified VacA and recombinant VacA (rVacA) induced apoptosis (21, 40) that was via a mitochondria-dependent pathway, stimulating cytochrome c release (28, 65). To the contrary, Caputo *et al.* reported that VacA was associated with *H. pylori*-induced VEGF up-regulation, which depends on the activation of the EGFR and MAP kinase cascade (18). The exclusive role of VacA in apoptosis, therefore, may be questionable.

Epidemiological studies have shown that gastric cell damage is associated with disruption of cytoskeletal structure (26,62) and reactive oxygen species (ROS) (10, 16). The protection of cells against them is a pivotal mechanism for cell survival. In the meanwhile, the gastritis induced by *H.pylori* infection stimulates the generation of ROS by the inflammatory cells present in the mucosa, resulting in gastric cell apoptosis which is strongly associated with atrophic gastritis and gastric cancer (20, 39, 44, 57, 71). By multivariate logistic regression analysis, the association of VacA with risk of glandular atrophy and intestinal metaplasia was increased in *H.pylori*-positive mucosa in our unpublished data. Thus, we need to investigate how VacA contributes to the pathogenesis of gastric mucosa after *H.pylori* infection in relation to MAP kinase pathways which mediate proliferation, differentiation, apoptosis and stress (9, 17, 23, 36, 72).

Superoxide dismutases (SOD) are essential enzymes that eliminate superoxide radical and hence protect cells from damage induced by free radicals (33). Loss of SOD-1 leads to

severe damage of mitochondria in neuroblastoma cell (5), senescence in cultured fibroblasts and apoptotic cell death in HeLa cells (12) as well as in spinal neurons (59).Villin, an actin binding protein, is an important marker of the pre-neoplastic cell type and induces enhanced motility and remodeling of the actin cytoskeleton contributing to the wound healing and cell proliferation (56). Mice deficient for the villin gene can organize microvilli in brush border but limits the severing of actin filaments in response to cellular injury, resulting in a deficiency in wound repair and cell motility, therefore end up cell death in response to chronic injury (8, 51).

Herein, we show that the activation of the MAP kinase cascade upon VacA stimuli could subsequently trigger changes in SOD-1 and villin expression and effect on cellular apoptosis and proliferation.

MATERIALS AND METHODS

Helicobacter pylori strains and culture conditions

Helicobacter pylori ATCC 49503 (strain 60190) and ATCC 43504 (NCTC 11637), wild-type, cytotoxic, cagA-positive strains with the vacA genotype s1/m1; ATCC 51932 (Tx30a), a wild type, cagA-negative with the vacA genotype s2/m2 (6) were purchased from American Type Culture Collection (Manassas, VA, USA). *H. pylori* were inoculated on Mueller Hinton agar plates supplemented with 5% horse serum. The plates were incubated for 2~3 days at 37 °C in a humidified 5% CO_2 incubator.

Cell line culture conditions

AGS human gastric epithelial cells (KCLB 21739) purchased from Korean Cell Line Bank (KCLB) were grown in RPMI 1640 medium supplemented with 10% FBS (Invitrogen Co. USA), 1% penicillin-streptomycin and 1% antibiotic-antimycotic at 37 °C in a 5% CO_2 incubator.

Polymerase chain reaction and plasmid construction

Primers were designed to amplify a vacA fragment encoding the mature VacA (43) from *H. pylori* strain ATCC 49503 (GeneBank accession No.: U05676). The sequences of sense primer with an NdeI site and antisense primer with a XhoI site were 5'-ggaattcCATATGTTTTTTACAACCGTGATCA-3' and 5'-ccgCTCGAGAGCGTAGCTAGCGAAA-3', respectively. The parameters for PCR were 94 °C for 2min, ×1; 94 °C for 30s, 45 °C for 30s, 68 °C for 2min, ×10; 94°C for 30s, 45 °C for 30s,

68 °C for 2min+5s increase per cycle, ×20; 68 °C for 7min, ×1. The resulting PCR product was digested with NdeI and XhoI and ligated to the pET 41b (+) digested with above mentioned restriction enzymes to create plasmid pVAC953. The recombinant plasmid contains the vacA fragment encoding the mature VacA cytotoxin (amino acids 34 to 854, including the A34M substitution) with an octa-His tag at the carboxyl terminus was amplified in *E.coli* DH5' (ECOS 101). The insert DNA was analyzed with T7 promoter (5'-TAATACGACTCACTATAGGG-3') or T7 terminator (5'-GCTAGTTATTGCTCAGCGG-3') by a sequencing analyzer (Genotech. co., Daejeon, Korea).

Production of recombinant VacA

E.Coli BL21 (DE3) was transformed by 1 ng of pVAC953 and kanamycine-resistant clones were selected. One colony bearing pVAC953 was inoculated into 5mL of LB broth containing 30 μg/ml of kanamycine and grown at 37 °C overnight with shaking. The overnight cultures were diluted 1 to 100 into TB broth supplemented with 0.5 % glucose and 30 μg/ml of kanamycine, and incubated at 24 °C until they reached an optical density of 0.4-0.6 at 600 nm. These cultures were induced with 0.1 mM of IPTG and incubated at 24 °C for 20 hours more. *E.coli* soluble extracts were prepared as follows. Around 100 ml volume of IPTG-induced cultures were pelleted by centrifugation at 5000 rpm for 10 min and resuspended in a 20 ml of lysis buffer containing 20 mM Tris-HCl (pH 7.9), 0.5M NaCl, 5% glycerol, 0.5% NP40, protease inhibitor cocktail (Complete mini, Roche Co. Germany), 1mM PMSF (Roche Co. USA), and 0.5mg/ml egg white lysozyme (Sigma Co. USA). The bacterial suspensions were incubated for 30 min at room temperature and then treated with freezing at -70°C and thawing at 37°C three times. After

three successive rounds of freeze-thaw, DNase, RNase and $MgCl_2$ were added to a final concentration of 20 μg/ml, 10 μg/ml and 10 mM, respectively. The bacterial suspensions were incubated on ice for 30 min and then sonicated for 1min (Sonics & Materials, Inc. Vibra Cell, pulse; 2s, Amp; 30W). The bacterial lysate were centrifuged at 12000 × g for 10 min at 4°C to remove insoluble cell debris. The supernatant was used for purification using His-Bind affinity chromatography (Novagen Co. USA). The purification of rVacA toxin was performed according to manufacture's protocol. Briefly, the first pool of fractions eluted with 0.5 M imidazole by His-Bind column chromatography were reloaded into another His-Bind column equilibrated with 20 mM Tris-HCl (pH7.9) supplemented with 0.5 M NaCl, 0.02% NP-40, 0.2% glycerol and 0.1M imidazole. The eluate with 0.5 M imidazole by the second chromatography was dialyzed against PBS and used in this study as a recombinant vacuolating cytotoxin.

Production of the polyclonal anti-rVacA antibodies raised in rabbit

New Zealand White rabbits were immunized with intradermal injections of 50 μg of rVacA, mixed with Freund's adjuvant. Immunoglobulins were purified by using rProtein G-Agarose (GibcoBRL, USA). This immunoglobulin recognized VacA in immunoblot not only with the ~89 kDa s1/m1 type but also with the ~92 kDa s2/m2 type.

Assay for vacuolating activity and cell viability

Vacuolating activity was assessed according to Cover *et al.*(22). Briefly, cells were seeded at 2-5×10^4 cells per well into 96-well plates and were grown overnight. The grown cells were washed with PBS and overlaid with a serum-free culture medium in the presence or absence of 10 mM

NH_4Cl to which *H. pylori* saline extract or *H.pylori* culture broth were added. Then cells were incubated for varying time at 37°C in a 5% CO_2 incubator. If necessary, the cells were incubated with rVacA for varying time or with varying concentrations. After incubation for indicated time, cell vacuolation was examined by inverted light microscopy and quantified by a neutral red uptake assay. Cell viability was determined by the MTS (3-(4,5-dimethylthiazol-2-yl)-5-(3-carboxymethoxy-phenyl)-2(4-sulfophenyl)-2H-tetrazolium, inner salt) assay (Promega Co. USA) or the MTT (3-(4,5-dimethylthiazol-2-yl)-2,5-diphenyltetrazolium bromide) assay (Roche Co. Germany), according to the manufacturer's protocols.

***H. pylori* saline extracts (HSE) and VacA enrichment by partial purification as native VacA sample**

Saline extracts were prepared by harvesting bacteria (ATCC49503) in 0.9 % of NaCl from a 36 h ~ 48 h blood agar culture. The suspensions were gently vortexed and centrifuged at 4000 rpm for 15 min at 4 °C and then filtered with a 0.22 μm syringe filter. In some experiments, HSE was pre-incubated for 1 hr on ice with neutralizing anti-VacA antibody before addition to the cells. Alternatively, HSE was immuno-depleted by pre-incubation for 1 hr on ice with neutralizing anti-VacA sera or non-immunized sera and protein A Sepharose (Invitrogen co.). After removal of immune complexes by centrifugation, the supernatant was tested for residual activity. For partial purification of VacA, HSE was precipitated with ammonium sulfate at 50% saturation, centrifuged for 20 min, 4 ºC, at 12000 rpm. The pellet was dissolved in 50 mM Tris-HCl (pH 8.0) and then dialyzed against two changes of 50 mM sodium phosphate (pH 6.0) at 4°C , re-precipitated materials were removed using centrifugation and loaded onto CM-sephadex

(Pharmacia co.) pre-equilibrated in phosphate buffer (pH 6.0). After a column chromatography, VacA was mainly existed in unbound fractions which was devoid of albumin and used for native VacA, designated as 'nVacA'. nVacA was immunodepleted of CagA by incubation with anti-CagA antibody C-300 bound to Protein A sepharose (Santa Cruz biotechnology Inc.) and then filter sterilized using a 0.2-μm filter.

AGS cells exposed to various *H.pylori* or VacA samples

Subconfluent monolayer of AGS cells on a 6-well plate was co-cultured for 5h with *H. pylori* in the presence or absence of anti-rVacA antibodies in a serum-free medium containing 10 mM NH_4Cl and then the cells were lysed in a 2 × SDS sample buffer. The effect of rVacA was assessed by AGS cells treated with indicated amounts of rVacA for various incubation periods in the presence or absence of anti-rVacA antibody or NH_4Cl. If necessary, anti-VacA antibody, 5-nitro-2-(3-phenylpropyl-amino) benzoic acid (NPPB), PD98059 or SB203580 was pretreated for 30 min prior to addition of rVacA. The lysed cells were subjected to SDS-PAGE and immunoblot.

Immunoblot analysis

Samples were separated by SDS-PAGE, transferred to Immobilin-P membrane (Milipore Co. USA). The membranes were blocked for 1 h with 3% BSA in TBST (10mM Tris-HCl, pH8.0, 150mM NaCl, 0.05% Tween 20) followed by incubating with primary antibody at a appropriate dilution in TBST containing 3% BSA overnight at 4°C. After washing three times with TBST for 10 min each, the membranes were incubated for 1 h with secondary antibody conjugated with horseradish peroxidase. Signals were amplified by the enhanced chemiluminescence system

(Pierce Co. USA) and exposed to X-ray film (Kodak Co. USA).

Immunoblot analysis of β–actin, Bax, Bcl-2, pERK1/2, ERK2, pp38, p38, SOD-1, β-tubulin and villin in AGS cells exposed to various *H.pylori* or rVacA

The effect of *H.pylori* infection or rVacA on the expressions of β–actin, Bax, Bcl-2, pERK1/2, ERK2, pp38, p38, SOD-1, β-tubulin and villin were assessed by AGS cells treated with various VacA samples with respective antibody; anti-β-actin, anti-Bax, anti-Bcl-2, anti-ERK2, and anti-p38 (Santa Cruz Biotechnology, Inc. USA), anti-villin (Chemicon, USA), anti-Cu/Zn SOD (Stressgene, USA), anti-pERK1/2, anti-pp38 (Cell signaling, USA) and anti-β-tubulin (Sigma Co. USA).

DAPI staining

The induction of apoptosis of cells by rVacA was assessed by DAPI (4',6'-diamidino-2-phenylindole) (Roche-Boehringer, Mannheim, Germany) staining. In brief, the cells on a slide glass were fixed with 4% paraformaldehyde followed by washing with PBS and staining with a 1 μg/ml DAPI solution for 10 min. The slides were then viewed under a fluorescence microscope (Nikon).

FITC-immunofluorescence staining of AGS cells

rVacA with or without anti-VacA antibody treated AGS cells were washed in PBS, fixed with cold acetone for 10min at room temperature, and then washed in PBS for three times. Anti-villin antibody (1:50) were incubated for 1 h at room temperature, washed in PBS for three times

followed by incubation with the fluorescein isothiocyanate (FITC)-conjugated anti-mouse secondary antibodies (National Veterinary Research & Quarantine Service, Korea) for 30 min at 37°C. After washing, the cover slips were mounted on the glass microscope slide with a drop of 50% glycerol PBS solution (pH 8.0). The cells were analyzed using an Olympus fluorescence microscope.

Microscopic imaging

Cells were visualized with TMS phase-contrast inverted microscopes (Nikon, Japan). Images were edited using Adobe PhotoShop 7.0 and Power Point.

RESULTS

Comparative analysis of the activity of native and recombinant VacA inducing vacuolation and apoptosis

After incubation for 8 h, rVacA increased neutral red (NR) uptake in AGS cells in a dose-dependent manner up to 0.8 μg/ml but decreased at higher concentration (Fig. 1 A). After AGS cells were incubated with indicated concentrations of rVacA for 24 h in serum-free media, cell viability was measured according to the ability of living cells to reduce the uncolored MTS substrate to a colored product (Fig. 1 C). As shown in Fig 1 C, rVacA induced mild dose-dependent apoptosis in AGS cells. To compare the activity of rVacA to that of native version, the vacuolation and apoptosis by native protein using HSE were assessed (Fig. 1 B and 1 D). The concentration of VacA in HSE was determined from the rVacA standard by antigen capture ELISA. The concentration of VacA corresponed to aproximately 1 % of the total protien of HSE (data not shown). As shown in Fig. 1B, however, the vacuolating activity of 50 μg/ml of HSE coincided with that of 0.8 μg/ml of rVacA. From the result, the activity of rVacA was supposed to be around 60% of that of native. While the vacuoles induced by native VacA were formed less than 4 h after addition of HSE and maintained during incubation for 10-20 h, and filled the entire cytoplasm, those induced by rVacA were formed slowly, somewhat defective and localized at the late endosomes. Furthermore, the perinuclear vesicles aggregates appeared to be collapsed, implying rVacA might disrupt actin cytoskeleton structure (Fig. 1 E).

Epithelial cell vacuolation and apoptosis induced by VacA

In order to confirm the role of VacA in *H.pylori*-induced apoptosis, AGS cells were treated with various VacA preparations (Fig.2 A). VacA-immunodepleted HSE showed significaltly reduced VacA level by approximately 70% of control while non-immunized sera did not change the VacA level of HSE treated. ERK1/2 signal was activated differently according to the various VacA preparations, wherein ERK1/2 activation by s1m1 vacA HSE without anti-VacA antibody was higher than in any other HSE treated AGS cells during a 2-h period (Fig. 2 B). Vacuolating activity of HSE was increased with incubation time up to 8 h and then decreased during 8-20 h of incubation (Fig. 2 C). Cell viability was inversely proportional to vacuolating activity and the level of VacA (Fig. 2 C and 2 D). The cell viability of AGS cells treated with s1/m1 vacA HSE was higher than that of AGS cells treated with VacA-depleted or PBS control at the incubation time of 4 h but it was decreased than VacA-reduced HSE or HSE plus anti-VacA antibody at the incubation of 20 h, suggesting that VacA induces not only cell proliferation at early time but also cell death of the AGS cells after prolonged exposure to it.

Comparative analysis of morphological change and protein expression of AGS cells co-cultured with various *H.pylori* strains

Epidemiological studies have shown that gastric cell damage infected with *H.pylori* is associated with disruption of cytoskeletal structure (62, 26) and reactive oxygen species (ROS) (10, 16). In order to determine the role of VacA in gastric cell damage by *H.pylori* infection, the level of SOD-1, a ROS scavenger enzyme and villin, an actin-binding protein were assessed in AGS cells co-cultured for 5 h with *H.pylori.* AGS cells infected with ATCC 49503 showed extensive cell vacuolation, disruption of cell–cell contacts and altered cell morphology (Fig. 3 A). The level of

VacA protein corresponded with the degree of vacuolation of AGS cells (Fig. 3 A and 3 B). These two strains have same vacA allelic type (s1m1 type) but different cagA subtype; CagA phosphorylation site is “A-B-C” in ATCC49503, “A-B-C-C-C” in HpKm. *H.pylori* induced ERK activation independently of the vacA type or the presence of cagA. But the level of ERK activation was the highest in AGS cells treated with ATCC49503. The levels of SOD-1 was slightly decreased in AGS cells with toxic VacA positive strains and the level of villin was slightly decreased in ATCC 49503 or ATCC 51932 treated AGS cells. (Fig. 3 B and 3 C).

Time course comparison of ERK1/2, SOD-1 and villin expression upon s1m1 HSE

ATCC49503 induced ERK activation and decreased SOD-1 and villin expression compared to negative control. Next, we investigated the effects of VacA on those protein expressions depending on incubation time using HSE of ATCC49503. The HSE activated ERK1/2 at 1 h and lasted thereafter in a time-dependent manner over an 8-h period (Fig. 4). SOD-1 expression was increased at 1 h and reached maximal at 2 h and decreased thereafter in a time -dependent manner. Villin was decreased in a time-dependent manner by 1 h and then re-induced thereafter. ERK activation appeared to be associated with the increase in SOD-1 expression and the decrease in villin expression at 1 h.

p38 MAPK and Bax mediate rVacA-induced apoptosis and requirement of ERK activation for cell survival

To confirm the significance of ERK1/2, SOD-1 and villin in VacA-induced apoptosis, we investigated cellular expression of those proteins including Bax, Bcl2, and p38 upon functional

rVacA stimulation. AGS cells treated with rVacA during varying incubation times were analyzed for DNA damage, ERK and p38 activation, Bax, Bcl2, villin and SOD-1 expression (Fig. 5 A – 5 C). As shown in Fig. 5 A, nucleus condensation and fragmentation were found in DAPI-stained AGS cells at 16 h. The extent of DNA fragmentation was determined by a direct counting of the number of apoptotic nuclei (Fig. 5 B). As shown in Fig. 5C, ERK1/2 activation induced by rVacA exhibited a biphasic time course, the early component peaking at 30 min and the late component at 4 h and then considerably reduced after a 16 h-incubation. Phosphorylation of p38 was maximal at 4 h, maintained until 8 h and declined abruptly at 16 h. The expression of villin was increased at 1 h and declined thereafter, whereas SOD-1was decreased after 1 h, and then re-increased during 4-8 h and then declined markedly at 16 h. The results of Bax expression using anti-Bax antibody showed that the expression level of approximately 18 kDa band was complementary to that of a 43 kDa band. The 18kDa band was decreased markedly at 8 h and 16 h while a 43 kDa band was increased abruptly at corresponding times. Bax is a pro-apoptotic protein and exists as a monomer in the cytosol. However, it translocates to the mitochondria, where it forms oligomers after an apoptotic stimulus (4). Thus, these data indicate that an 18 kDa band is a Bax monomer and a 43kDa band is a Bax dimer. Reportedly, the activation of p38 in response to environmental stress and inflammatory cytokines can result in apoptosis (37). Pro-apoptotic signals such as Bax dimerization and p38 activation were induced promptly after stimulation by rVacA. At the same time, a defense mechanism such as antioxidant protein and a component of cytoskeletal structure was also induced. Cell viability maintained during 8 h incubation with rVacA with sustained phospho-ERK1/2 and Bcl2 but the balance was disrupted during 8-16 h with Bax dimerization, resulting in cell death. At 16 h, only the expression of Bax

dimer was increased while those of others were decreased, which shows Bax dimerization plays critical role for apoptosis induced by rVacA. In addition, activation of p38 MAPK appeared to precede Bax dimerization in rVacA-induced apoptosis.

rVacA induced Bax dimerization in a dose dependent manner

After 4 h treatment with the indicated concentration of rVacA, ERK1/2 activation in AGS cells occurred with maximal activation at 5 to 10 μg/ml of rVacA. At 20 μg/ml, rVacA, however, decreased ERK1/2 phosphorylation (Fig. 6 A upper). Bax dimerization by rVacA was increased in a dose-dependent manner (Fig. 6 A). The addition of anti-VacA antibody attenuated the Bax dimerization of 5-10 μg of rVacA but not higher concentrations of rVacA (Fig. 6 B). On the contrary, as shown in Fig. 2B, anti-VacA antibody did not inhibit rVacA-induced ERK1/2 activation.

Effect of NPPB and anti-VacA antibody on VacA-induced phospho-ERK1/2, SOD-1 and villin

A nonspecific chloride channel blocker, NPPB, can inhibit the channel activity of VacA, resulting in a reduction of vacuolation and cytochrome c release caused by VacA (14). NPPB suppressed expression of phospho-ERK1/2 and villin at 0.2 μg/ml of VacA and 2μg/ml of rVacA (Fig. 7 A and 7 B) implying that anionic channel formation of VacA may be associated with ERK1/2 activation and villin expression. While ERK activation by native VacA but not by rVacA was slightly decreased in the presence of anti-VacA antibody, the level of SOD-1 induced by both native VacA and rVacA was unlikely to change with anti-VacA antibody. The level of villin,

however, was significantly reduced under the presence of anti-VacA antibody (Fig. 7 A and 7 B). Cell viability depending on incubation time showed that upon 0.2 μg of VacA stimulation, cell viability decreased up to 5h, re-increased up to 10h and then decreased thereafter. VacA may induce cell apoptosis followed by cell proliferation to compensate for cell loss wherein SOD-1 and villin might be involved via ERK1/2 activation. Whereas NPPB did not show significant effects on cell viability, anti-VacA antibody protected cells from VacA intoxication and lasted by 20h. rVacA, however, decreased net cell viability in a time-dependent manner and, contrary to Fig. 7 C, NPPB protected moderately but not significantly cell from rVacA intoxication. Anti-VacA antibody protected cell from rVacA induced cell death by 10h but could not at 20h. The differences between nVacA and rVacA may be caused by the crudity of nVacA which might have a proliferating factor.

rVacA induces SOD-1 via ERK activation and phosphorylation of p38 in AGS

We investigated a possible role of MAP kinases in VacA-induced SOD-1 and villin expression using MAP kinases inhibitor. After 16 h incubation with rVacA, the expression of SOD-1 was increased compared to negative control and, however, PD98059 inhibited that induction of SOD-1, suggesting that the induction by rVacA is via ERK1/2 activation (Fig. 8 A). The level of villin remained at 1 μg/ml of rVacA and severely suppressed at 2 μg/ml rVacA thereafter, irrelevant to treatment of anti-rVacA antibody or PD98059. The activation of p38 by rVacA was in a dose-dependent manner while anti-rVacA antibody attenuated the phosphorylation of p38 in AGS cells treated with 2 μg of rVacA to a similar extent of negative control. Next, the effect of rVacA on cell viability with an MTT assay was assessed. The cytotoxic effect of rVacA was measured after

16 h of incubation with 0-4 μg of rVacA (Fig. 8 B). Cell viability was decreased in a dose-dependent manner when AGS cells were treated with rVacA in the presence or absence of PD98059 ($P < 0.05$, Kruskal-Wallis test). There is, however, almost no effect on cell viability after incubation with rVacA in the presence of anti-rVacA antibody, with only a slight decrease in cell viability at higher doses (4 μg of rVacA). PD98059, which totally abrogated ERK1/2 activation in the AGS cells, significantly decreased cell viability compared to control but the rate of cell death at the indicated concentrations of rVacA was similar to that induced by rVacA only.

Inhibition of the p38 pathway protects the AGS cells partially from rVacA-induced apoptosis and activates ERK1/2

The involvement of p38 in the VacA-induced apoptosis in AGS cells was confirmed using SB203580, a specific inhibitor of p38. Although, SB203580 did not completely inhibit the cytotoxic activity of rVacA, it did protect the cells partially from rVacA-induced apoptosis, which may be at least, partially associated with ERK1/2 activation in AGS cells treated with the p38 inhibitor (Fig. 9 A and 9 B). These results imply that there may be a mutual induction between the two pathways: one leading to inhibit, and the other to promote apoptosis, especially against rVacA cytotoxicity in AGS cells. Increased SOD-1 expression was likely to be associated with increased ERK phosphorylation and in part, decreased p38 phosphorylation in the presence of anti-VacA antibody or SB203580 (Fig. 9 A).

Inhibition of p38 MAP kinase with SB203580 suppresses villin and Bcl2 expression

Despite cytoprotective effect, SB203580 was unlikely to prevent VacA-induced Bax dimerization

(Fig. 10). But higher level of SB203580 (60 μM), partially inhibited rVacA-induced Bax dimerization, implying that inhibition of p38 MAP kinase activity may not directly lead to the inhibition of VacA-induced Bax activation. Interestingly, SB203580 inhibited the expression of Bcl2 and villin expression, indicating p38 may play a role in cell proliferation or differentiation for survival upon VacA insult. In accordance with Fig. 9 A, VacA-induced SOD-1 expression was not inhibited by SB203580 and furthermore, prevented SOD-1 reduction from the higher dose of rVacA. The results indicate that VacA-induced p38 MAPK activation is not only involved in apoptosis but also involved in survival mechanism.

Inhibition of p38 MAP kinase accelerates rVacA-induced apoptosis after exposure to H_2O_2.

To further confirm the role of MAP kinases in response to ROS induced by rVacA, we investigated the effects of H_2O_2, product of SOD enzymatic reaction on rVacA-induced apoptosis in the absence or presence of MAP kinase inhibitor or anti-VacA antibody. SB203580 protected AGS cells partially from rVacA-induced apoptosis as shown in Fig. 9 which appeared to be associated with ERK1/2 activation and SOD-1 expression after 16 h incubation. However, it accelerated cell death of AGS cells treated with rVacA for 4 h after exposure to both 50 and 100 μM H_2O_2 for 1 h (Fig. 11 B and 11 C). On the contrary, PD98059 slightly protected cell from rVacA and 100 μM of H_2O_2 intoxication (Fig. 11 C). Therefore, p38 MAP activation may play a critical role in cellular protection in the early stage of response to oxidative stress and conversely, ERK activation promotes oxidative stress- or H_2O_2-induced apoptosis in the early stage which may trigger cell proliferation thereafter.

Anti-VacA antibody blocks the localization of villin to contractile actin ring

Villin expression in response to VacA or rVacA was very versatile but Anti-VacA antibody strongly inhibited villin expression, so we identified the villin expression and localization using an immunofluorescent staining. Villin was mainly observed in contractile actin ring of dividing cells (Fig. 12 A). Contractile actin ring, comprised of non-muscle myosin II and actin filaments assembles equatorially at the cell cortex, driving plasma membrane invagination from the cortex (2). In microvilli, near the perinuclear compartment and microtubules, was villin identified but contractile ring was not seen nearly in AGS cells treated with anti-VacA antibody with or without rVacA (Fig. 12 B).

DISCUSSION

Apoptosis of gastric epithelial cells induced by *H.pylori* infection is strongly associated with the development of glandular atrophy and intestinal metaplasia (57, 58). VacA has been considered as an apoptosis-inducing factor both in vivo and in vitro (66). Although the activation of MAP kinases induced by VacA has been demonstrated (14, 18, 45), the involvement in apoptotic event is not clear. Our results showed that the activation of ERK1/2 and p38 by rVacA was link to cell survival and apoptosis, differentially (67, 68).

VacA induces clustering and perinuclear redistribution of late endosomes which requires a functional microtubule cytoskeleton (41). rVacA also reached late endosomes but could not induce extensive vacuolar structure and fill the entire cytoplasm. After reaching the compartment, rVacA may attack cytoskeleton structure which may be causes of defective and localizing vacuolation in perinuclear compartment wherein structure collapsed. It could be a cause of reduced villin level after high dose ($\geq$ 2μg/ml) or/and prolonged exposure to rVacA, leading to induction of cell cycle arrest and apoptosis. However, rVacA stimulated villin expression at early stage, implying it may be necessary for inducing vacuolation and morphological change. Villin, an actin binding protein is associated with the actin bundles that support microvilli, bundles, caps, nucleates, and severs actin (7,15, 55). As shown in Fig. 12, we have shown that villin is localized in contractile actin ring during late anaphase and disappeared gradually according to completion of cell division wherein it may sever actin ring. Anti-VacA antibody might suppress cell division by inhibiting villin expression, which may be a cause of the abrupt cell death in AGS cells treated with rVacA plus anti-VacA antibody at 20h (Fig. 7 B). NPPB, an chloride channel blocker, inhibits VacA-induced vaculation and its internalization (30) and its inhibition of villin

expression induced by VacA or rVacA may be associated with the decrease in VacA-induced polymerization of actin due to blocking the membrane trafficking (29, 30). Villin is known to an important marker of the pre-neoplastic cell type, therefore the increase or decrease in the expression of it by VacA suggests VacA may play a role in gastric cancer development. Thus more verification on the role of VacA in regulating of villin is required.

Activation of p38 and accompanying decrease in a phspho-ERK1/2 level coincided with an increase in Bax dimer, a decrease in Bcl2 and apoptosis of AGS cells. rVacA-induced Bax dimerization and its association with apoptosis was coincided with the result of Yamasaki *et al*. (70). Inhibition of ERK1/2 by PD98059 decreased cell viability but was unlikely to potentiate the cytotoxic effect of rVacA. However, ERK1/2 activation contributed to sustaining cell survival for a limited time. While anti-VacA antibody inhibited p38 activation and Bax dimerization induced by rVacA, it was unlikely to inhibit ERK1/2 and SOD expression, which may contribute to the ability of the antibody to protect cells from cell death by rVacA intoxication. These results indicated that effect of VacA on ERK1/2 and p38 activation may be differentially regulated, of which only one is dependent on initial membrane binding of VacA which is inhibited by anti-VacA antibody but is independent of internalization of VacA. Reportedly, EGF receptor, lipid rafts, and receptor protein tyrosine phosphatase beta have been proposed as VacA receptor, suggesting that VacA may bind to multiple sites on the cell surface (49). Therefore, VacA-induced signal transduction may be different depending on a kind of recepor bound.

ERK inhibition by PD98059 did not aggravate or abolish the cell death induced by rVacA; however, it did inhibit the induction of SOD-1 by rVacA as shown in Fig. 8. Obst *et al*. have shown that *H.pylori* extract directly induces the synthesis of ROS in gastric epithelial cells

and causes DNA damage (47). Induction of SOD-1 by toxic VacA enriched sample or rVacA implies that VacA may stimulate ROS production, probably from the mitochondria or from MAP kinase activation (72). Recent work described VacA enhances PGE2 production through induction of COX-2 mRNA in a time- and dose-dependent manner via p38 MAP kinase activation in AZ-521 cells (33), which may induce ROS production. Protection of cells against ROS is accomplished through the activation of oxygen-scavenging enzymes such as SOD, catalase and glutathione peroxidase (61). The superoxide anion-scavenging activity of SOD-1 leads to an increase in H_2O_2, which may induce catalase expression. AGS cells treated with rVacA with MAP kinase inhibitors showed rVacA increased catalase expression moderately, ERK inhibitor decreased the expression slightly and p38 inhibitor (SB203580) did not affect the VacA-induced catalase expression. However, there were no significant differences in the expression level of catalase compared to that of SOD-1 (data not shown). Without a concomitant increase in peroxide-scavenging enzymes, excess H_2O_2 might be involved in the cell damage caused by VacA. Activation of ERK has been shown to promote or block H_2O_2-dependent apoptosis (69, 73). In the present work, H_2O_2 accelerated rVacA-induced cell death, especially, in p38 inhibitor pre-treated AGS cells, suggesting p38 MAP kinase play a pivotal role in protection against H_2O_2-induced cell death (11, 27) and, conversely, ERK1/2 aggravates H_2O_2 -induced cell death.

Van Laethem *et al.* reported that activation of p38 by UVB required for the translocation of Bax to the mitochondria in human keratinocytes (64). Association of p38 with rVacA-induced apoptosis in our results was based on the effect of SB203580 on AGS cells treated with rVacA, resulting in the attenuation of cell death. However, despite cytoprotective effect of SB203580, inhibition of p38 MAPK activation was unlikely to reduce Bax dimerization induced by rVacA

and furthermore, leaded to decrease in Bcl2 and villin expression. Nakayama et al.(46) reported that VacA activates p38 signal pathway which is independent of cytochrome c release from mitochondria caused by VacA in AZ-521 cells. Pleiotropic activity of p38 MAPK such as proliferation, differentiation and survival upon a stimulus may be explained by the existence of several p38 MAPK isomers with distinct functions (23, 54, 3). According to some literatures, p38 promotes but p38β inhibits apoptosis, and both p38 isomers are suppressed by SB203580 (52, 35, 63). From this, we deduce that SB203580 may not only protect cell from cell death via p38α but also suppress host defense mechanism via p38β in response to VacA intoxication. Among p38 isomers, p38α has been more abundantly expressed and active than other isoforms (32). According to the paper of Abdollahi *et al.* (1), mRNA expression of p38α appears to be constant but p38β to be induced at 16 h and maintained over a 24-h period without any stress. In the presence of some stress, however, expression of p38β was induced at 8 h, maximal at 16 h and then declined thereafter. Therefore differential activation of p38α and p38β MAP kinase coupled with ERK activation may result in various phenotypic consequences in response to VacA intoxication. Taken together, these results indicated that there is an antagonistic regulation between ERK1/2 and p38 on VacA-induced apoptosis. These antagonistic regulations on taxol-induced apoptosis and nitric oxide-induced apoptosis have been described (38, 60). Thus, the roles of ERK and p38 MAPKs in apoptosis or proliferation might be dependent on cell type and state (19).

In addition, Ranganathan *et al*., demonstrated that Mn-SOD dependent H_2O_2 production leads to the activation of the ERK1/2 signaling and subsequent downstream transcriptional increases in MMP-1 expression which is involved in extracellular matrix remodeling (53).

Therefore, it is likely that VacA-induced ROS stimulates ERK1/2-dependent SOD-1 expression by which H_2O_2 production might lead to another ERK1/2 activation and subsequent downstream transcriptional increases in MMPs expression which may be involved in actin cytoskeleton-degradation, leading to apoptosis. Recent report by Pillinger *et al*, suggests that *H. pylori* induced MMP-1 secretion is CagA-dependent and –independent which are regulated via ERK positively and p38 MAPK negatively (50). Thus, the association of VacA with MMP-1 secretion needs investigating further.

Apoptosis in gastric epithelium by *H.pylori* infection and ROS production have been associated with the incidence of gastric cancer. Moreover, Lin *et al.* reported in a case-control study (41) that higher SOD-1 levels may be associated with an increased risk of gastric cancer. *H.pylori*-associated gastritis is predominant in the antrum where a significant increase of the SOD activity has been detected (24, 25). Malignant cells produce active superoxide, which makes the cancer cell highly dependent on SOD for survival and thus more sensitive to inhibition of SOD, hence Huang *et al*, suggested targeting SOD may be a promising approach to the selective killing of cancer cells (34).

In summary, we first demonstrated that VacA stimulates expression of SOD-1 via ERK1/2 activation and the expression and degradation of villin using recombinant VacA. These results suggest that SOD-1 and villin are expressed differentially upon VacA insult depending on dose and exposure time via ERK and p38 MAP kinases; decrease in SOD-1 and villin expression coupled with Bax dimerization leads to apoptosis of gastric epithelial cells. Therefore, VacA may be a crucial factor of gastric cancer development in subjects with chronic *H.pylori* infection by a repeated stimulation of cellular proliferation and apoptosis mediated by a fine-tuned control

between ERK and p38 MAP kinase.

GRANTS

This research was supported by a grant (CBM31-B3003-01-01-00) from the Center for Biological Modulators of the 21st Century Frontier R & D Program, the Ministry of Science and Technology, Korea.

REFERENCE

1. **Abdollahi T, Robertson NM, Abdollahi A, Litwack G**. Inhibition of TRAIL-induced apoptosis by IL-8 is mediated by the p38-MAPK pathway in OVCAR3 cells. *Apoptosis* 10(6):1383-1393, 2005.

2. **Albertson R, Riggs B, Sullivan W.** Membrane traffic: a driving force in cytokinesis. *Trends Cell Biol* 15(2): 92-101, 2005.

3. **Alonso G, Ambrosino C, Jones M, Nebreda AR.** Differential activation of p38 mitogen-activated protein kinase isoforms depending on signal strength. *J Biol Chem* 275(51): 40641-40648, 2000.

4. **Antonsson B, Montessuit S, Sanchez B, Martinou JC.** Bax is present as a high molecular weight oligomer/complex in the mitochondrial membrane of apoptotic cells. *J Biol Chem* 276: 11615–11623, 2001.

5. **Aquilano K, Vigilanza P, Rotilio G, Ciriolo MR.** Mitochondrial damage due to SOD1 deficiency in SH-SY5Y neuroblastoma cells: a rationale for the redundancy of SOD1. *FASEB J* 20(10):1683-1685, 2006.

6. **Atherton JC, Cao P, Peek RM Jr, Tummuru MK, Blaser MJ, Cover TL**. Mosaicism in vacuolating cytotoxin alleles of *Helicobacter pylori*: association of specific vacA types with cytotoxin production and peptic ulceration. *J Biol Chem* 270: 17771-17777, 1995.

7. **Athman R, Louvard D, Robine S.** The epithelial cell cytoskeleton and intracellular trafficking. III. How is villin involved in the actin cytoskeleton dynamics in intestinal cells? *Am J Physiol Gastrointest Liver Physiol* 83: G496-G502, 2002

8. **Athman R, Louvard D, Robine S.** Villin enhances hepatocyte growth factor-induced actin cytoskeleton remodeling in epithelial cells. *Mol Biol Cel* 14(11):4641-4653, 2003.

9. **Avruch J.** MAP kinase pathways: The first twenty years. *Biochim Biophys Acta*. doi:10.1016/j.bbamcr.2006.11.006, 2006.

10. **Baik SC, Youn HS, Chung MH, Lee WK, Cho MJ, Ko GH, Park CK, Kasai H, Rhee KH.** Increased oxidative DNA damage in *Helicobacter pylori*-infected human gastric mucosa. *Cancer Res* 56: 1279-1282, 1996.

11. **Bao M, Lou Y.** Isorhamnetin prevent endothelial cell injuries from oxidized LDL via activation of p38MAPK. *Eur J Pharmacol* 547(1-3):22-30, 2006.

12. **Blander G, de Oliveira RM, Conboy CM, Haigis M, Guarente L**. Superoxide dismutase 1 knock-down induces senescence in human fibroblasts. *J Biol Chem* 278(40): 38966-38969, 2003.

13. **Blaser MJ, Perez-Perez GI, Kleanthous H, Cover TL, Peek RM, Chyou PH**, **Stemmermann GN, Nomura A**. Infection with *Helicobacter pylori* strains possessing cagA is associated with an increased risk of developing adenocarcinoma of the stomach. *Cancer Res* 55:2111–2115, 1995.

14. **Boncristiano M, Paccani SR, Barone S, Ulivieri C, Patrussi L, Ilver D, Amedei A, D'Elios MM, Telford JL, Baldari CT.** The *Helicobacter pylori* vacuolating toxin inhibits T cell activation by two independent mechanisms. *J Exp Med* 198: 1887-1897, 2003.

15. **Bretscher A, Weber K.** Villin: the major microfilament-associated protein of the intestinal microvillus. *Proc Natl Acad Sci* 76: 2321-2325, 1979.

16. **Briede JJ, Pot RG, Kuipers EJ, van Vliet AH, Kleinjans JC, Kusters JG.** The presence of the cag pathogenicity island is associated with increased superoxide anion radical scavenging activity by *Helicobacter pylori*. *FEMS Immunol Med Microbio* 44: 227-232, 2005.

17. **Brown L, Benchimol S**. The involvement of MAPK signaling pathways in determining the cellular response to p53 activation: cell cycle arrest or apoptosis. *J Biol Chem* 281: 3832-3840. 2006.

18. **Caputo R, Tuccillo C, Manzo BA, Zarrilli R, Tortora G, Blanco Cdel V, Ricci V, Ciardiello F, Romano M**. *Helicobacter pylori* VacA toxin up-regulates vascular endothelial growth factor expression in MKN 28 gastric cells through an epidermal growth factor receptor-, cyclooxygenase-2-dependent mechanism. *Clin Cancer Res* 9: 2015-2021, 2003.

19. **Chang L, Karin M.** Mammalian MAP kinase signaling cascades. *Nature* 410: 37-40, 2001.

20. **Correa P.** Does *Helicobacter pylori* cause gastric cancer via oxidative stress? *Biol Chem* 387: 361-364, 2006.

21. **Cover TL, Krishna US, Israel DA, Peek RM Jr**. Induction of gastric epithelial cell apoptosis by *Helicobacter pylori* vacuolating cytotoxin. *Cancer Res* 63: 951-957, 2003.

22. **Cover TL, Puryear W, Pérez-Pérez GI, Blaser MJ.** Effect of urease on HeLa cell vacuolation induced by *Helicobacter pylori* cytotoxin. *Infect Immun* 59: 1264-1270, 1991.

23. **Ding M, Shi X, Dong Z, Chen F, Lu Y, Castranova V, Vallyathan V.** Freshly fractured

crystalline silica induces activator protein-1 activation through ERKs and p38 MAPK. *J Biol Chem* 274: 30611-30616, 1999.

24. **Farkas R, Pronai L, Tulassay Z, Selmeci L.** Relationship between eradication of *Helicobacter pylori* and gastric mucosal superoxide dismutase activity. *Anticancer Res* 25(6C): 4763-4767, 2005.

25. **Farkas R, Selmeci L, Tulassay Z Pronai L.** Superoxide-dismutase activity of the gastric mucosa in patients with *Helicobacter pylori* infection. *Anticancer Res* 23(5b): 4309-4312, 2003.

26. **Frisch SM, Francis H.** Disruption of epithelial cell-matrix interactions induces apoptosis. *J Cell Biol* 124: 619-626, 1994.

27. **Gaitanaki C, Pliatska M, Stathopoulou K Beis I.** Cu2+ and acute thermal stress induce protective events via the p38-MAPK signalling pathway in the perfused Rana ridibunda heart. *J Exp Biol* 210(Pt 3): 438-446, 2007.

28. **Galmiche A, Rassow J, Doye A, Cagnol S, Chambard JC, Contamin S, de Thillot V, Just I, Ricci V, Solcia E, Van Obberghen E, Boquet P.** The N-terminal 34 kDa fragment of *Helicobacter pylori* vacuolating cytotoxin targets mitochondria and induces cytochrome c release. *EMBO J* 19: 6361-6370, 2000.

29. **Gauthier NC, Monzo P, Gonzalez T, Doye A, Oldani A, Gounon P, Ricci V, Cormont M Boquet P.** Early endosomes associated with dynamic F-actin structures are required for late trafficking of *H. pylori* VacA toxin. *J Cell Biol* 177(2): 343-354, 2007.

30. **Gauthier NC, Ricci V, Gounon P, Doye A, Tauc M, Poujeol P Boquet P.** Glycosylphosphatidylinositol-anchored proteins and actin cytoskeleton modulate

chloride transport by channels formed by the *Helicobacter pylori* vacuolating cytotoxin VacA in HeLa cells. *J Biol Chem* 279(10): 9481-9489, 2004.

31. **Gebert B, Fischer W, Weiss E, Hoffmann R, Haas R.** *Helicobacter pylori* Vacuolating Cytotoxin Inhibits T Lymphocyte Activation. *Science* 301: 1099-1102, 2003.

32. **Hale KK, Trollinger D, Rihanek M, Manthey CL.** Differential expression and activation of p38 mitogen-activated protein kinase alpha, beta, gamma, and delta in inflammatory cell lineages. *J Immunol* 162(7): 4246-4252, 1999.

33. **Hisatsune J, Yamasaki E, Nakayama M, Shirasaka D, Kurazono H, Katagata Y, Inoue H, Han J, Sap J, Yahiro K, Moss J, Hirayama T.** *Helicobacter pylori* VacA enhances prostaglandin E(2) production through induction of cyclooxygenase 2 expression via a p38 mitogen-activated protein kinase/activating transcription factor 2 cascade in AZ-521 cells. *Infect Immun* 75(9): 4472-4481, 2007.

34. **Huang P, Feng L, Oldham EA, Keating MJ, Plunkett W.** Superoxide dismutase as a target for the selective killing of cancer cells. *Nature* 407(6802): 390-395, 2000.

35. **Huang Q, Bu S, Yu Y, Guo Z, Ghatnekar G, Bu M, Yang L, Lu B, Feng Z, Liu S, Wang F.** Diazoxide prevents diabetes through inhibiting pancreatic beta-cells from apoptosis via Bcl-2/Bax rate and p38-beta mitogen-activated protein kinase. *Endocrinology* 148(1): 81-91, 2007.

36. **Kapur R, Chandra S, Cooper R, McCarthy J, Williams DA.** Role of p38 and ERK MAP kinase in proliferation of erythroid progenitors in response to stimulation by soluble and membrane isoforms of stem cell factor. *Blood* 100: 1287-1293, 2002.

37. **Keates S, Keates AC, Warny M, Peek RM Jr, Murray PG, Kelly CP.** Differential

activation of mitogen-activated protein kinases in AGS gastric epithelial cells by cag+ and cag- *Helicobacter pylori*. *J Immunol* 163: 5552-5559, 1999.

38. **Kim SJ, Ju JW, Oh CD, Yoon YM, Song WK, Kim JH, Yoo YJ, Bang OS, Kang SS, Chun JS.** ERK-1/2 and p38 kinase oppositely regulate nitric oxide-induced apoptosis of chondrocytes in association with p53, caspase-3, and differentiation status. *J Biol Chem* 277: 1332-1339, 2002.

39. **Konturek PC, Kania J, Konturek JW, Nikiforuk A, Konturek SJ, Hahn EG.** *H. pylori* infection, atrophic gastritis, cytokines, gastrin, COX-2, PPAR gamma and impaired apoptosis in gastric carcinogenesis. *Med Sci Monit* 9: SR53-SR66. 2003.

40. **Kuck D, Kolmerer B, Iking-Konert C, Krammer PH, Stremmel W, Rudi J.** Vacuolating cytotoxin of *Helicobacter pylori* induces apoptosis in the human gastric epithelial cell line AGS. *Infect Immun* 69: 5080-5087, 2001.

41. **Li Y, Wandinger-Ness A, Goldenring JR, Cover TL.** Clustering and redistribution of late endocytic compartments in response to *Helicobacter pylori* vacuolating toxin. *Mol Biol Cell* 15(4): 1946-1959, 2004.

42. **Lin Y, Kikuchi S, Obata Y, Yagyu K**; Tokyo Research Group on Prevention of Gastric Cancer. Serum copper/zinc superoxide dismutase (Cu/ Zn SOD) and gastric cancer risk: a case-control study. *Jpn J Cancer Res* 93: 1071-1075, 2002.

43. **McClain MS, Cover TL.** Expression of *Helicobacter pylori* vacuolating toxin in *Escherichia coli*. *Infect Immun* 71: 2266-2271, 2003.

44. **Mizuki I, Shimoyama T, Fukuda S, Liu Q, Nakaji S, Munakata A.** Association of gastric epithelial apoptosis with the ability of *Helicobacter pylori* to induce a neutrophil

oxidative burst. *J Med Microbio* 49: 521-524, 2000.

45. **Nakayama M, Hisatsune J, Yamasaki E, Nishi Y, Wada A, Kurazono H, Sap J, Yahiro K, Moss J, Hirayama T.** Clustering of *Helicobacter pylori* VacA in lipid rafts, mediated by its receptor, receptor-like protein tyrosine phosphatase beta, is required for intoxication in AZ-521 Cells. *Infect Immun* 74: 6571-6580, 2006.

46. **Nakayama M, Kimura M, Wada A, Yahiro K, Ogushi K, Niidome T, Fujikawa A, Shirasaka D, Aoyama N, Kurazono H, Noda M, Moss J, Hirayama T.** *Helicobacter pylori* VacA activates the p38/activating transcription factor 2-mediated signal pathway in AZ-521 cells. *J Biol Chem* 279: 7024-7028, 2004.

47. **Obst B, Wagner S, Sewing KF, Beil W.** *Helicobacter pylori* causes DNA damage in gastric epithelial cells. *Carcinogenesis* 21: 1111-1115, 2000.

48. **Pai P, Cover TL, Tarnawski AS.** *Helicobacter pylori* vacuolating cytotoxin (VacA) disorganizes the cytoskeletal architecture of gastric epithelial cells. *Biochem Biophys Res Commun* 262: 245-250, 1999.

49. **Papini E, Zoratti M, Cover TL.** In search of the *Helicobacter pylori* VacA mechanism of action. *Toxicon* 39(11): 1757-1767, 2001.

50. **Pillinger MH, Marjanovic N, Kim SY, Lee YC, Scher JU, Roper J, Abeles AM, Izmirly PI, Axelrod M, Pillinger MY, Tolani S, Dinsell V, Abramson SB, Blaser MJ.** *Helicobacter pylori* stimulates gastric epithelial cell MMP-1 secretion via CagA-dependent and -independent ERK activation. *J Biol Chem* 282(26): 18722-18731, 2007.

51. **Pinson KI, Dunbar L, Samuelson L, Gumucio DL.** Targeted disruption of the mouse villin gene does not impair the morphogenesis of microvilli. *Dev Dyn* 211(1): 109-121,

1998.

52. **Porras A, Zuluaga S, Black E, Valladares A, Alvarez AM, Ambrosino C, Benito M, Nebreda AR.** P38 alpha mitogen-activated protein kinase sensitizes cells to apoptosis induced by different stimuli. *Mol Biol Cell* 15(2): 922-33, 2004.

53. **Ranganathan AC, Nelson KK, Rodriguez AM, Kim KH, Tower GB, Rutter JL, Brinckerhoff CE, Huang TT, Epstein CJ, Jeffrey JJ, Melendez JA.** Manganese superoxide dismutase signals matrix metalloproteinase expression via H_2O_2-dependent ERK1/2 activation. *J Biol Chem* 276(17): 14264-14270, 2001.

54. **Recio JA, Merlino G.** Hepatocyte growth factor/scatter factor activates proliferation in melanoma cells through p38 MAPK, ATF-2 and cyclin D1. *Oncogene* 21: 1000-1008, 2002.

55. **Revenu C, Courtois M, Michelot A, Sykes C, Louvard D, Robine S.** Villin severing activity enhances actin-based motility in vivo. *Mol Biol Cell* 18(3): 827-838, 2007.

56. **Revenu C, Rafika A, Robine S, and Louvard D.** The co-workers of actin filaments: from cell structures to signals. *Nat Rev Mol Cell Biol* 5: 635-646, 2004.

57. **Rogers AB, Taylor NS, Whary MT, Stefanich ED, Wang TC, Fox JG.** *Helicobacter pylori* but not high salt induces gastric intraepithelial neoplasia in B6129 mice. *Cancer Res* 65(23): 10709-15, 2005.

58. **Romano M, Ricci V, Zarrilli R.** Mechanisms of disease: *Helicobacter pylori*-related gastric carcinogenesis--implications for chemoprevention. *Nat Clin Pract Gastroenterol Hepatol* 3(11): 622-632, 2006.

59. **Rothstein JD, Bristol LA, Hosler B, Brown RH Jr, Kuncl RW.** Chronic inhibition of

superoxide dismutase produces apoptotic death of spinal neurons. *Proc Natl Acad Sci U S A* 91(10): 4155-4159, 1994.

60. **Seidman R, Gitelman I, Sagi O, Horwitz SB, Wolfson M.** The role of ERK1/2 and p38 MAP-kinase pathways in taxol-induced apoptosis in human ovarian carcinoma cells. *Exp Cell Res* 268: 84-92, 2001.

61. **Smoot DT, Elliott TB, Verspaget HW, Jones D, Allen CR, Vernon KG, Bremner T, Kidd LC, Kim KS, Groupman JD, Ashktorab H.** Influence of *Helicobacter pylori* on reactive oxygen-induced gastric epithelial cell injury. *Carcinogenesis*. 21: 2091-2095, 2000.

62. **Su B, Ceponis PJ, Sherman PM.** Cytoskeletal rearrangements in gastric epithelial cells in response to *Helicobacter pylori* infection. *J Med Microbiol* 52(Pt 10): 861-867, 2003.

63. **Tourian L Jr, Zhao H, Srikant CB.** p38alpha, but not p38beta, inhibits the phosphorylation and presence of c-FLIPS in DISC to potentiate Fas-mediated caspase-8 activation and type I apoptotic signaling. *J Cell Sci* 117(Pt 26): 6459-6471, 2004.

64. **Van Laethem A, Van Kelst S, Lippens S, Declercq W, Vandenabeele P, Janssens S, Vandenheede JR, Garmyn M, Agostinis P**. Activation of p38 MAPK is required for Bax translocation to mitochondria, cytochrome c release and apoptosis induced by UVB irradiation in human keratinocytes. *FASEB J* 18: 1946-1948, 2004.

65. **Willhite DC, Blanke SR.** *Helicobacter pylori* vacuolating cytotoxin enters cells, localizes to the mitochondria, and induces mitochondrial membrane permeability changes correlated to toxin channel activity. *Cell Microbiol* 6: 143-154, 2004.

66. **Willhite DC, Cover TL, Blank SR.** Cellular Vacuolation and Mitochondrial

Cytochrome c Release Are Independent Outcomes of *Helicobacter pylori* Vacuolating Cytotoxin Activity That Are Each Dependent on Membrane Channel Formation. *J Biol Chem* 278: 48204-48209, 2003.

67. **Woo CH, You HJ, Cho SH, Eom YW, Chun JS, Yoo YJ, Kim JH.** Leukotriene B(4) stimulates Rac-ERK cascade to generate reactive oxygen species that mediates chemotaxis. *J Biol Chem* 277(10): 8572-8578, 2002.

68. **Xia Z, Dickens M, Raingeaud J, Davis RJ, Greenberg ME.** Opposing effects of ERK and JNK-p38 MAP kinases on apoptosis. *Science* 270: 1326-1331. 1995.

69. **Xu Q, Konta T, Nakayama K, Furusu A, Moreno-Manzano V, Lucio-Cazana J, Ishikawa Y, Fine LG, Yao J, Kitamura M.** Cellular defense against H_2O_2-induced apoptosis via MAP kinase-MKP-1 pathway. *Free Radic Biol Med* 36(8): 985-993, 2004.

70. **Yamasaki E, Wada A, Kumatori A, Nakagawa I, Funao J, Nakayama M, Hisatsune J, Kimura M, Moss J, Hirayama T.** *Helicobacter pylori* vacuolating cytotoxin induces activation of the proapoptotic proteins Bax and Bak, leading to cytochrome c release and cell death, independent of vacuolation. *J Biol Chem* 281: 11250-11259, 2006.

71. **Yoshimura T, Shimoyama T, Tanaka M, Sasaki Y, Fukuda S, Mund nakata A.** Gastric mucosal inflammation and epithelial cell turnover are associated with gastric cancer in patients with *Helicobacter pylori* infection. *J Clin Pathol* 53: 532-536, 2000.

72. **Zhuang S, Schnellmann RG.** A death-promoting role for extracellular signal-regulated kinase. *J Pharmacol Exp Ther* 319: 991-997, 2006.

73. **Zhuang S, Yan Y, Daubert RA, Schnellmann RG.** Epiregulin promotes proliferation and migration of renal proximal tubular cells. *Am J Physiol Renal Physiol* 292(1): F440-

F447, 2007.

FIGURE LEGENDS

Fig. 1 Comparative analysis of the activity of recombinant and native VacA. *A*; vacuolating activities of rVacA were measured by a neutral red dye uptake assay in the absence (white column) or presence (black column) of 10 mM NH_4Cl. *B*; vacuolating activities of *H. pylori* saline extract (HSE) of ATCC 49503. Values represented the means and standard deviations from triplicate samples and the absorbance at 550 nm for neutral red dye uptake after subtracting the blank. *C*; concentration-dependent cell death induced by rVacA in AGS cells. *D*; concentration-dependent cell death induced by HSE. The cells were grown in 96-well plates (3.5×10^4 cells/well) for 24 h and changed a serum-free medium containing indicated quantities of rVacA or HSE in the absence (white column) or presence (black column) of 10 mM NH_4Cl followed by incubating for 8 h or 24 h. MTS cell proliferation colorimetric assay (Promega, USA) was used to quantify living cells. Values were obtained from the absorbance of the formazan at 492 nm, expressed as the percentages of relative to that of control without both VacA and NH_4Cl and represented the means and standard deviations from triplicate samples. $^{*}p < 0.05$, and $^{\dagger}p < 0.01$ (Student's *t*-test, compared with each result for cells without rVacA or HSE). *E*; formation of cellular vacuoles in response to HSE (left edge) and rVacA (right) in the presence of 10 mM NH_4Cl.

Fig. 2 Comparative analysis of cytotoxicity of various VacA. *A*; the effects of various VacA preparations on AGS cells were investigated. S2m2 VacA and s1m1 VacA were a HSE of ATCC51932 and ATCC49503, respectively. To get rid of VacA from HSE, s1m1 *vacA* HSE was

immunodepleted by preincubation for 1 hr on ice with neutralizing anti-VacA or non-immunized rabbit antibody bound to protein A-Sepharose. After removal of immune complexes by centrifugation, immunodepleted HSE with anti-VacA antibody (VacA-reduced s1m1 HSE) or non-immunized sera (s1m1 HSE+serum) was tested for residual activity. *B*; immunoblot analysis of phospho-ERK1/2 with 20 μg of AGS cells lysates after incubating for 2 h with the indicated VacA sample in the absence or presence of anti-VacA antibody. *C*; vacuolating activity depending on incubation time was measured by a neutral red dye uptake assay and *D*; an MTT cell proliferation colorimetric assay was used to quantify living cells. Values represent relative cell viability as a percentage of cells treated with PBS and the means and standard deviations from quadruplet samples. AGS cells were treated for 4 h, 8 h and 20 h with PBS as control, PBS plus anti-VacA, s1m1 *vacA* HSE, s1m1 *vacA* HSE plus anti-VacA, s2m2 *vacA* HSE, VacA-reduced s1m1 *vacA* HSE (immunodepleted with anti-sera against rVacA) or s1m1 HSE+serum (immunodepleted with non-immunized sera) in the presence of 10 mM NH_4Cl. $^{*}p < 0.05$, $^{\dagger}p < 0.01$ compared to control at indicated incubation time without anti-VacA antibody. $^{\#}p < 0.05$ compared to control with anti-VacA antibody.

Fig. 3 Effects of various *H.pylori* strains on the indicated protein expression in AGS cells. AGS cells were co-cultured with the indicated *H.pylori* stains for 5 h in a serum-free medium. After a 5 h incubation period, AGS cells were washed in PBS and then lysed with 2× SDS sample buffer. The lysed cells were assessed for CagA and VacA bound to cells by immunoblotting. *A*; The AGS cells transfected with ATCC 49503 were extensively vacuolated while about 50% of the AGS cells were vacuolated, when transfected with HpKm, an s1/m1 *vacA* genotype. Expectedly,

AGS cells infected with ATCC 51932 (s2/m2 *vacA/cagA*$^-$) were not vacuolated except vacuoles induced by NH_4Cl like negative control. *B*; A high level of VacA was produced by ATCC 49503(s1m1 *vacA/cagA*$^+$, western type, ABC) compared with that produced by HpKm. (s1m1 *vacA/cagA*$^+$, western type, ABCCC), which was in accordance with the extent of vacuolation by respective *H.pylori* strain. The lysed cells were assessed for phosphorylated ERK1/2, SOD-1, villin and β-tubulin by an immunoblotting. *C*; Relative expression level to β-tudetermined from Fig. 3B.

Fig. 4 Time course of protein expression in response to s1m1 HSE. *A*; AGS cells were treated with HSE of ATCC49503 in a serum-free medium and cells treated without HSE for 0 h. The time course of phosph-ERK1/2, SOD-1, and villin expression in response to HSE were determined using an immunoblotting over an 8 h period. *B*; Relative densities of phospho-ERK1/2 to ERK2 and of SOD-1 or villin to β- tubulin were measured using Image J software.

Fig. 5 rVacA-induced protein expression in AGS cells in a time-dependent manner. AGS cells were exposed to 10 μg/ml of rVacA for the indicating times over a 16-h period in a serum-free medium and cells treated without rVacA for 0 min. *A*; AGS cells were incubated in the above conditions and fixed with 2% paraformaldehyde in PBS, followed by staining with DAPI. The changes in nuclear morphology and DNA fragmentation were revealed in a time-dependent manner by DAPI staining. *B*; The histograms represent the percentage of apoptotic cells in AGS cells exposed to rVacA in a time course experiments. The values represent the means and standard deviations determined from three areas per specimen. *C*; Identification of the expression

of proteins at the indicated time point was by an immunoblot using antibodies for the corresponding proteins. Data are representative of at least two experiments.

Fig. 6 VacA-induced Bax dimerization in dose-dependent manner. *A*; AGS cells were incubated with indicated concentration of rVacA for 4 h and the cells were lysed in 2× SDS sample buffer. ERK activation and Bax dimerization in AGS cells were assessed using an immunoblotting in the absence or presence of anti-VacA antibody. *B*; relative densities of Bax dimer to β-tubuline after exposure of AGS cells to the indicated concentration of rVacA. The expression level of protein at zero concentration was induced by the filtrate by filtering rVacA through Microcon YM-50 (Millipore Co., USA) which has 50,000 daltons of cutoffs filter. The indicated concentration of rVacA was prepared by the combination of concentrated rVacA and the filtrate. Data are representative of at least two experiments.

Fig. 7 Effect of NPPB and anti-VacA antibody on VacA-induced protein expression. *A* and *B*; Subconfluent AGS cells were pre-treated with 50 μM NPPB for 30 min prior to stimulation with nVacA (*A*) (for detail, see 'Materials and Methods') or rVacA (*B*) for 5 h. Effect of anti-VacA antibody was determined by using a VacA sample pretreated with anti-VacA antibody for 30 min. The concentration of VacA out of nVacA was estimated by ELISA using rVacA as a standard. *C* and *D*; AGS cells were treated with 0.2 μg/ml of VacA or 5μg/ml of rVacA. Cell viability depending on incubation time was measured by an MTT cell proliferation colorimetric assay. The cell viability represents a percentage of the values of cells prior to stimulation of nVacA (*C*) or rVacA (*D*) and the means and standard deviations from triplet or quadruplet samples. $^{*}p < 0.05$,

$^{\dagger}p < 0.01$ vs values at 5h, $^{**}p < 0.05$, $^{\dagger\dagger}p < 0.01$ vs values at 10h, Student's *t*-test.

Fig. 8 Regulation of ERK1/2 and p38 MAPK in VacA-induced apoptosis and SOD-1 induction by rVacA via ERK activation. *A*; AGS cells were treated with the indicated concentration of rVacA for 16 h in the absence or presence of anti-rVacA antibody or un- or pretreated with PD98059. ERK1/2, p38 kinase and SOD-1 proteins were determined by an immunoblot analysis. Data are representative of at least two experiments. *B*; cell viability was assessed by an MTT assay in AGS cells treated with the same condition indicated in Fig. 8A. The value of viable cells is expressed as a percentage of untreated cells. Values represent the means and standard deviations from quintuplet samples. Data are representative of at least two experiments. rVacA samples were prepared by the combination of concentrated rVacA and the filtrate. $^{\dagger}p < 0.05$ vs non-treated with rVacA, $^{\ddagger}p< 0.01$ vs non-treated with rVacA and $^{*}p < 0.05$ vs 2 μg/ml rVacA treatment (Student's *t*-test).

Fig. 9 Effect of the inhibitor of p38 MAP kinases on SOD-1 expression and cell viability in AGS cells treated with rVacA. *A*; AGS cells were pre-incubated with or without indicated inhibitor (30 μM) for 30 min and then washed prior to adding 0-6 μg/ml of rVacA to cells. The cells were incubated for 8 h for protein expression by immunoblotting or *B*; for 16 h for cell viability by an MTT assay. rVacA decreased cell viability in a dose dependent manner ($^{\ddagger}p < 0.001$ vs non-treated with rVacA, $^{\dagger}p < 0.01$ vs 3 μg/ml rVacA treatment, Student's *t*-test). Anti-rVacA antibody and the p38 inhibitor SB 203580 partly protected AGS cells from rVacA-induced apoptosis ($^{*}p < 0.05$, $^{**}p < 0.01$ vs corresponding control, Student's *t*-test). The number of viable cells is expressed as

a percentage of untreated cells. Values represent the means and standard deviations from quintuplet samples. Data are representative of at least two experiments.

Fig. 10 Effect of p38 MAPK inhibition on Bax, Bcl2 and villin expression. AGS cells were pre-incubated with or without SB203580 for 30 min and then washed prior to adding 0-4 μg/ml of rVacA to cells. The cells were incubated for 12 h for the detection of protein expression by immunoblotting. Data are representative of at least two experiments.

Fig. 11 Inhibition of p38 MAP kinase accelerates rVacA-induced apoptosis after exposure to H_2O_2. Cell viability was assessed by an MTT assay in AGS cells treated with 0 to 4 μg/ml of rVacA for 4 h (*A*) or followed by exposure to 50 (*B*) or 100 μM H_2O_2 (*C*) for 1 h. The cell viability represents a percentage of the values of cells without stimulation of rVacA and exposure to H_2O_2 and the means and standard deviations from triplet or quadruplet samples. $^{*}p < 0.01$, $^{\dagger}p < 0.01$ vs non-treated with rVacA, $^{**}p < 0.05$, $^{\dagger\dagger}p < 0.01$ vs 2 μg/ml rVacA treatment and $^{\ddagger}p < 0.05$, $^{\ddagger\ddagger}p < 0.01$ vs negative control , Student's *t*-test.

Fig. 12 Immunofluorescent staining for villin in rVacA treated AGS cells. *A*; Villin is shown mainly in dividing cells, especially contractile ring (left panel) and cell nuclei was visualized by DAPI (right panel). Villin is strongly expressed in dividing cells (arrow) and then decreased after completion of cell cleavage (arrowhead). *B*; Villin is localized with actin in contractile ring and microtubules in rVacA treated AGS cells (left panel) but it is localized with actin in microvilli and in perinuclear compartment (right panel).

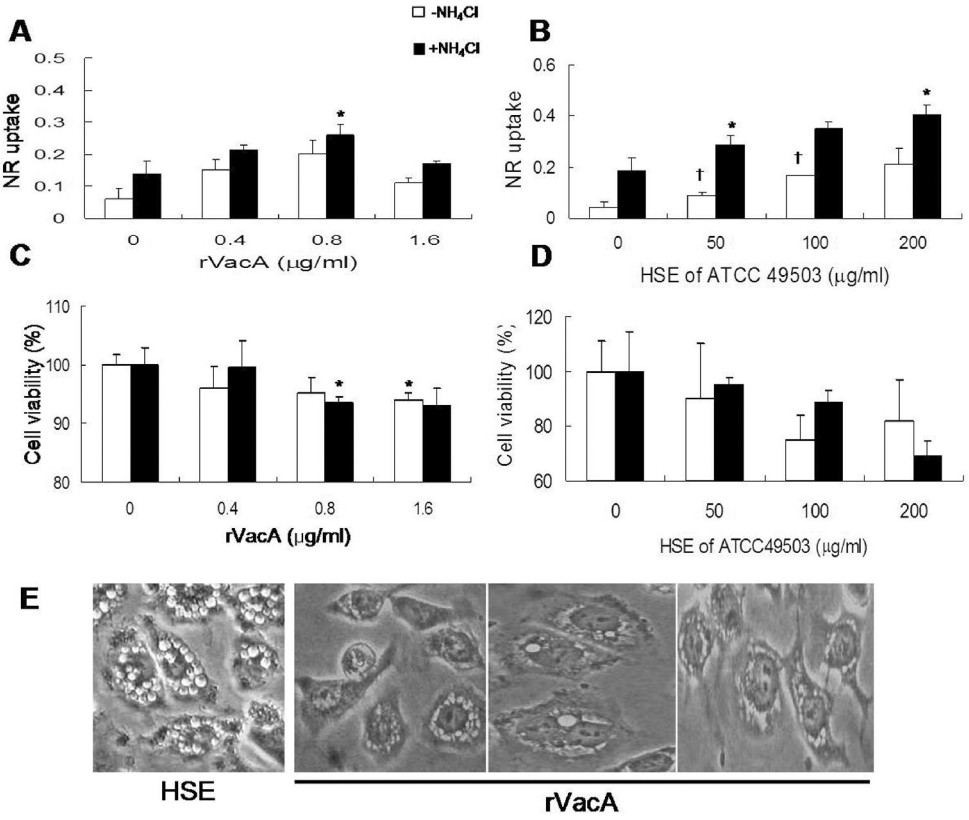

Fig. 1 Comparative analysis of the activity of recombinant and native VacA.
120x99mm (600 x 600 DPI)

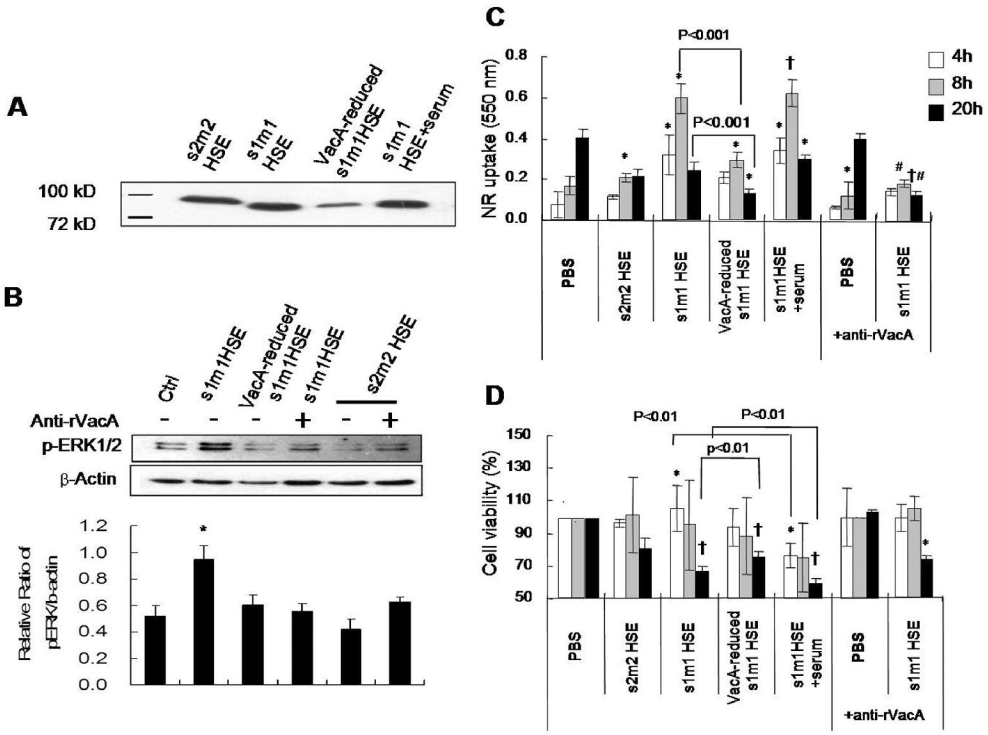

Fig. 2 Comparative analysis of cytotoxicity of various VacA.
120x90mm (600 x 600 DPI)

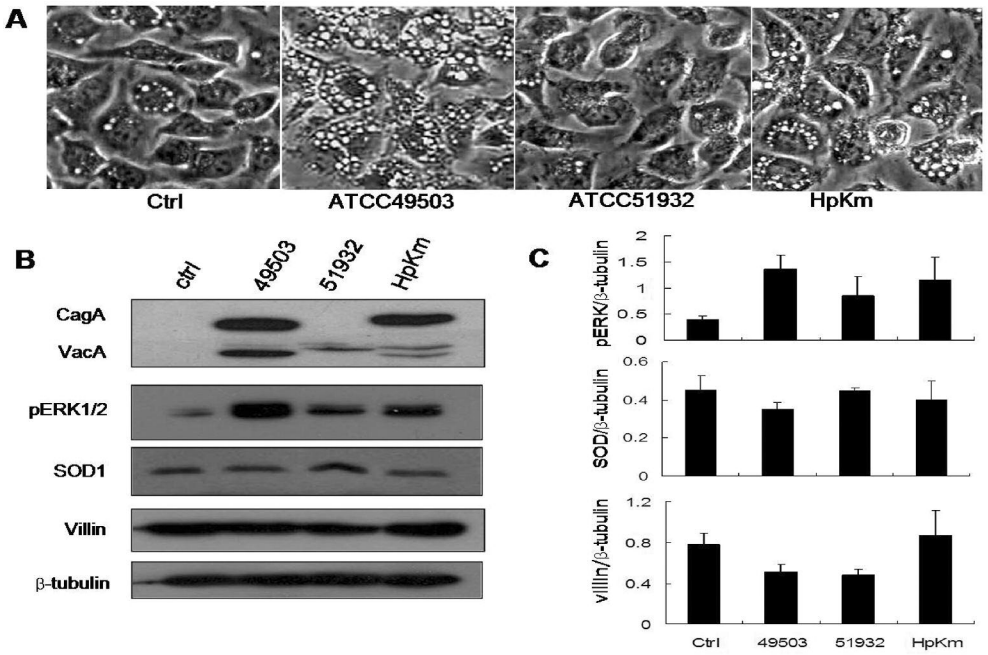

Fig. 3 Effects of various H.pylori strains on the indicated protein expression in AGS cells.
120x80mm (600 x 600 DPI)

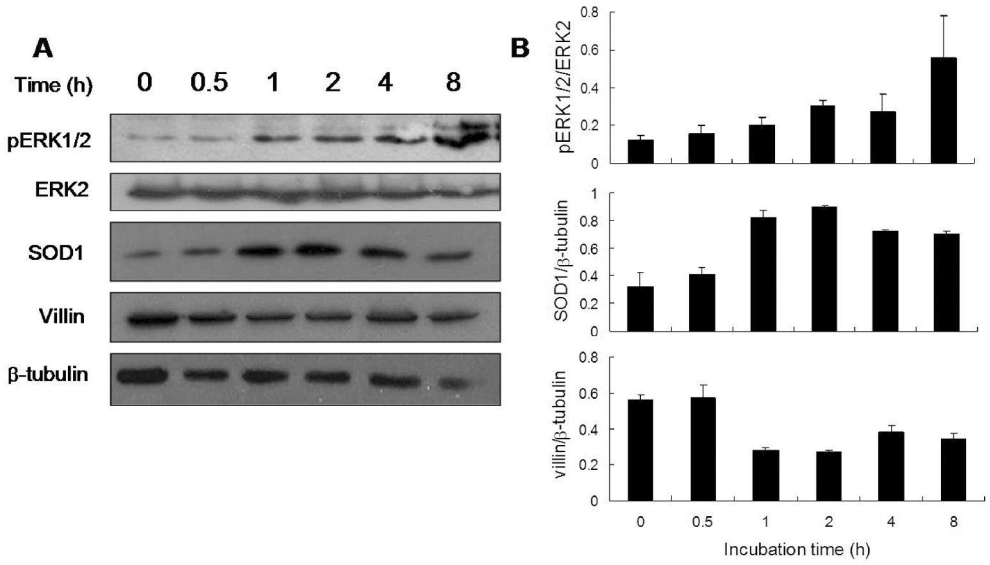

Fig. 4 Time course of protein expression in response to s1m1 HSE.
120x70mm (600 x 600 DPI)

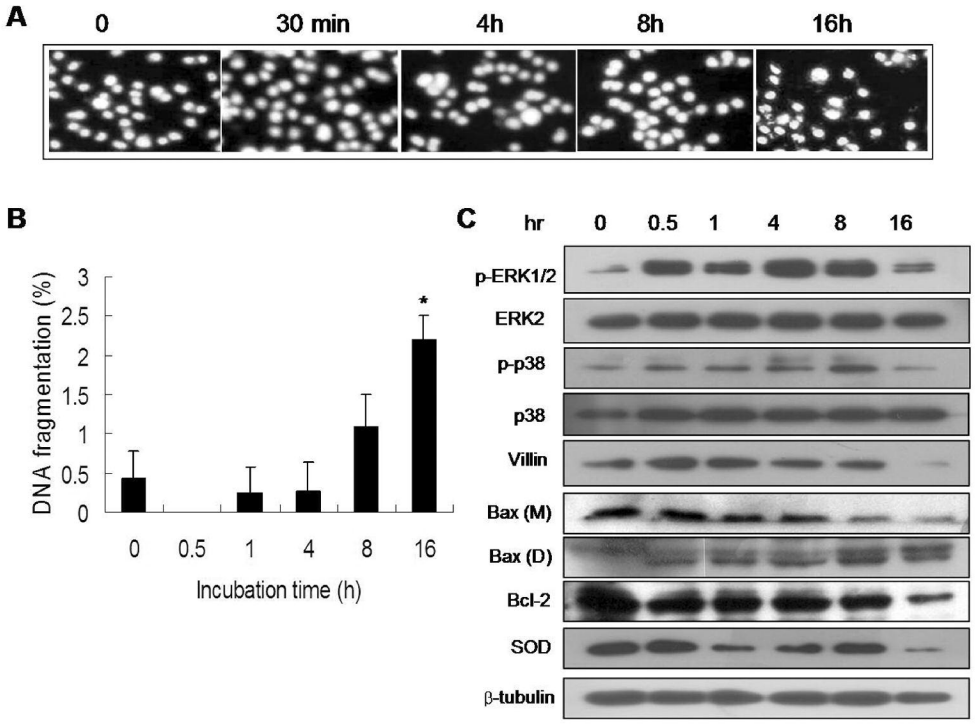

Fig. 5 rVacA-induced protein expression in AGS cells in a time-dependent manner.
120x90mm (600 x 600 DPI)

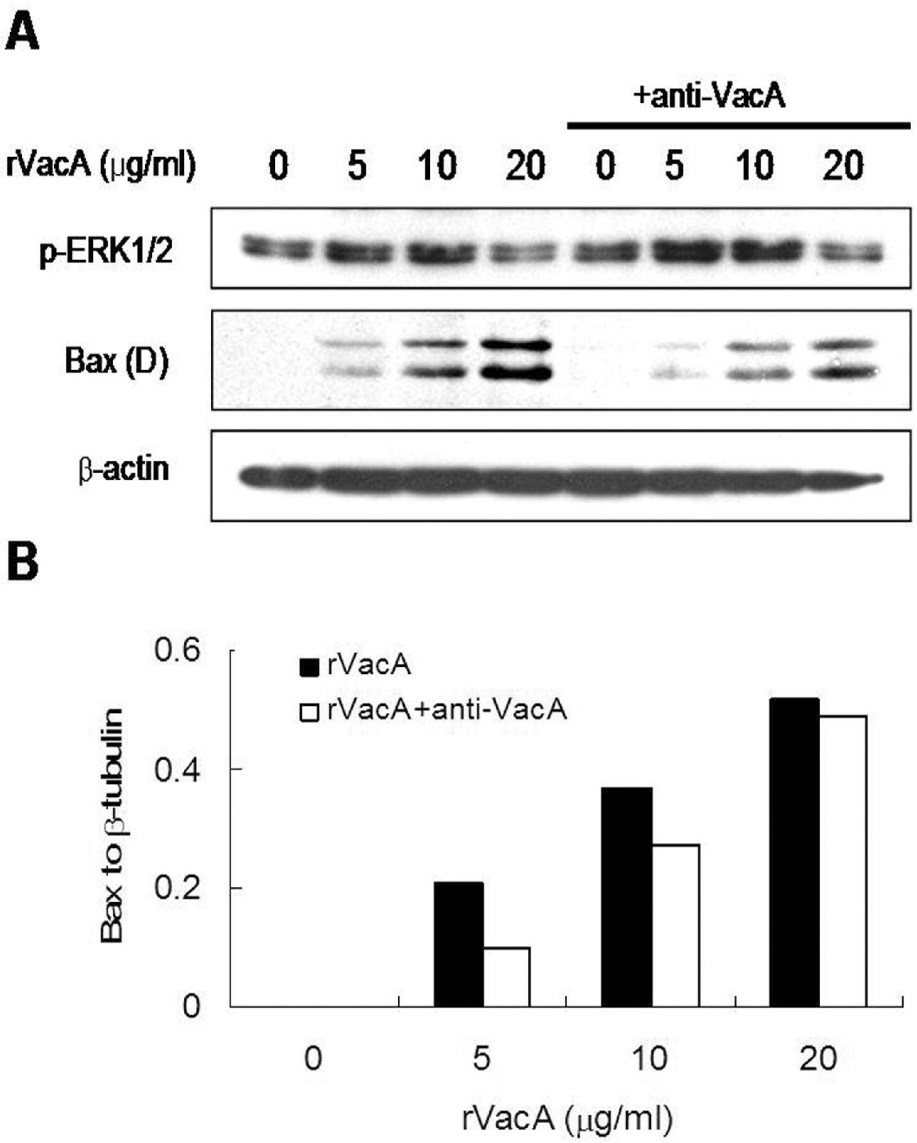

Fig. 6 VacA-induced Bax dimerization in dose-dependent manner.
80x99mm (600 x 600 DPI)

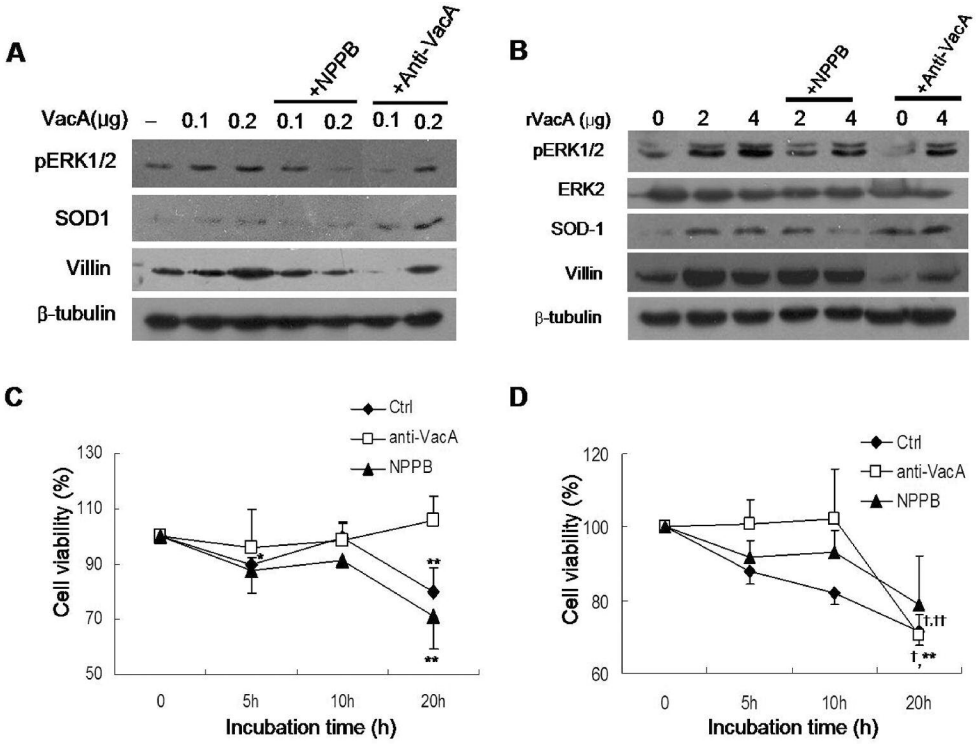

Fig. 7 Effect of NPPB and anti-VacA antibody on VacA-induced protein expression.
120x90mm (600 x 600 DPI)

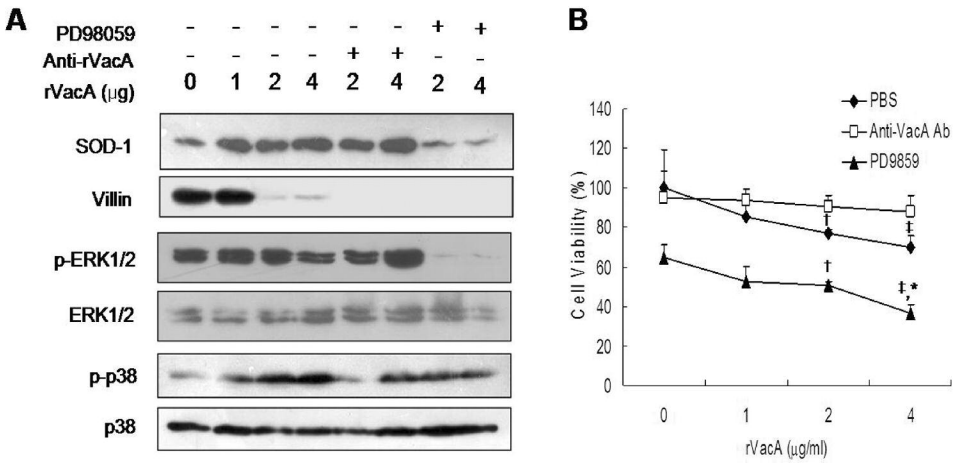

Fig. 8 Regulation of ERK1/2 and p38 MAPK in VacA-induced apoptosis and SOD-1 induction by rVacA via ERK activation.
120x59mm (600 x 600 DPI)

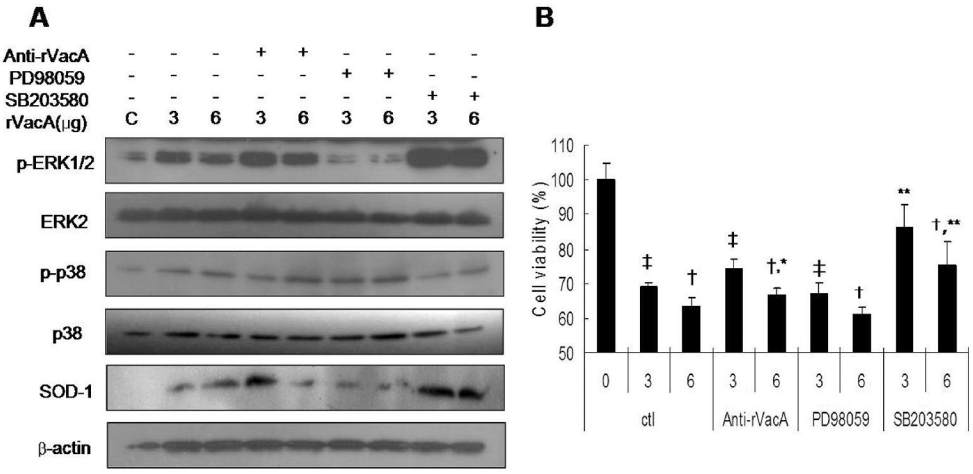

Fig. 9 Effect of the inhibitor of p38 MAP kinases on SOD-1 expression and cell viability in AGS cells treated with rVacA.
120x59mm (600 x 600 DPI)

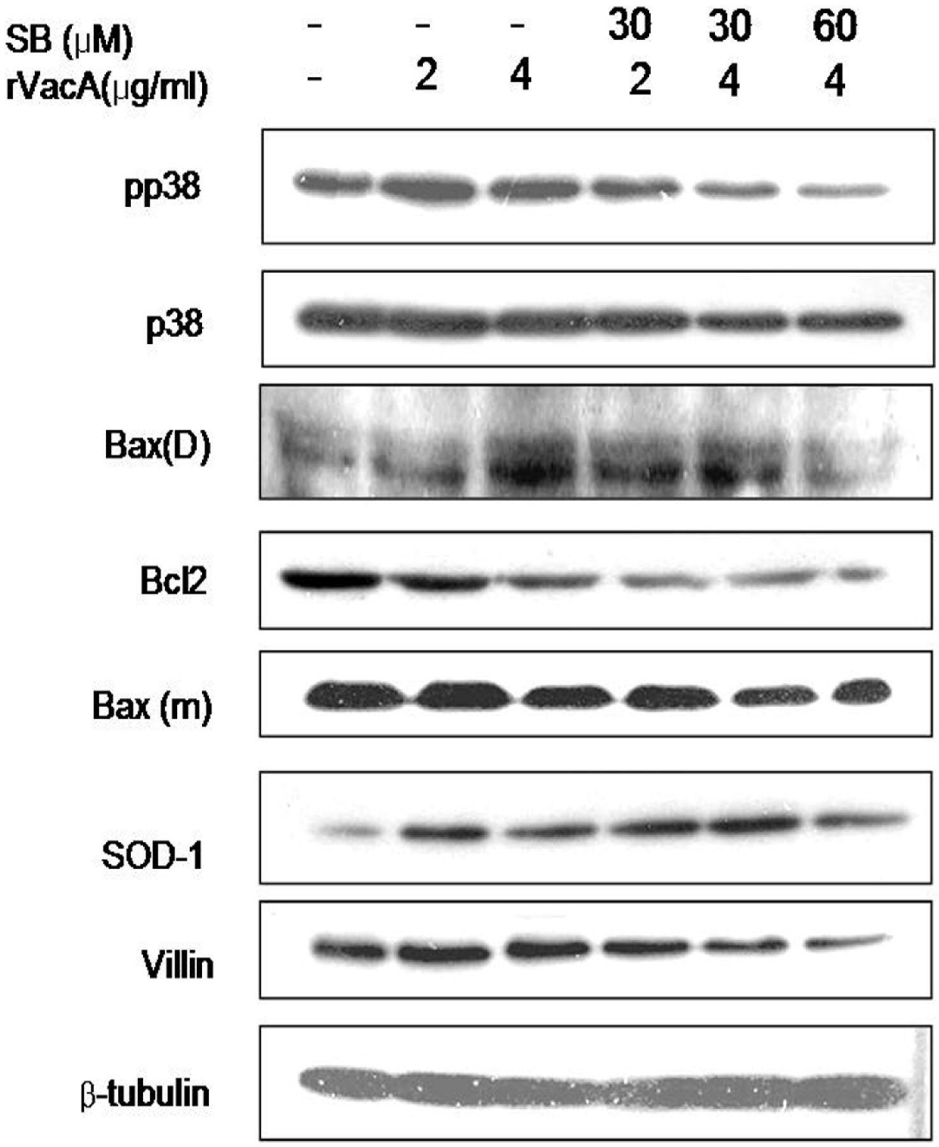

Fig. 10 Effect of p38 MAPK inhibition on Bax, Bcl2 and villin expression.
80x99mm (600 x 600 DPI)

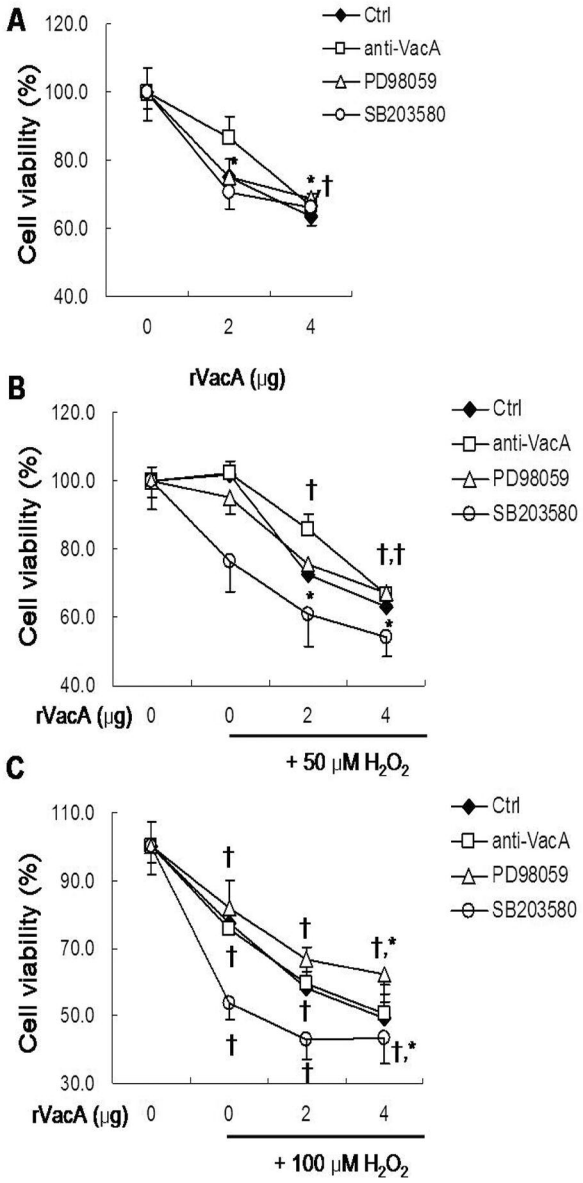

Fig. 11 Inhibition of p38 MAP kinase accelerates rVacA-induced apoptosis after exposure to H2O2.
80x160mm (600 x 600 DPI)

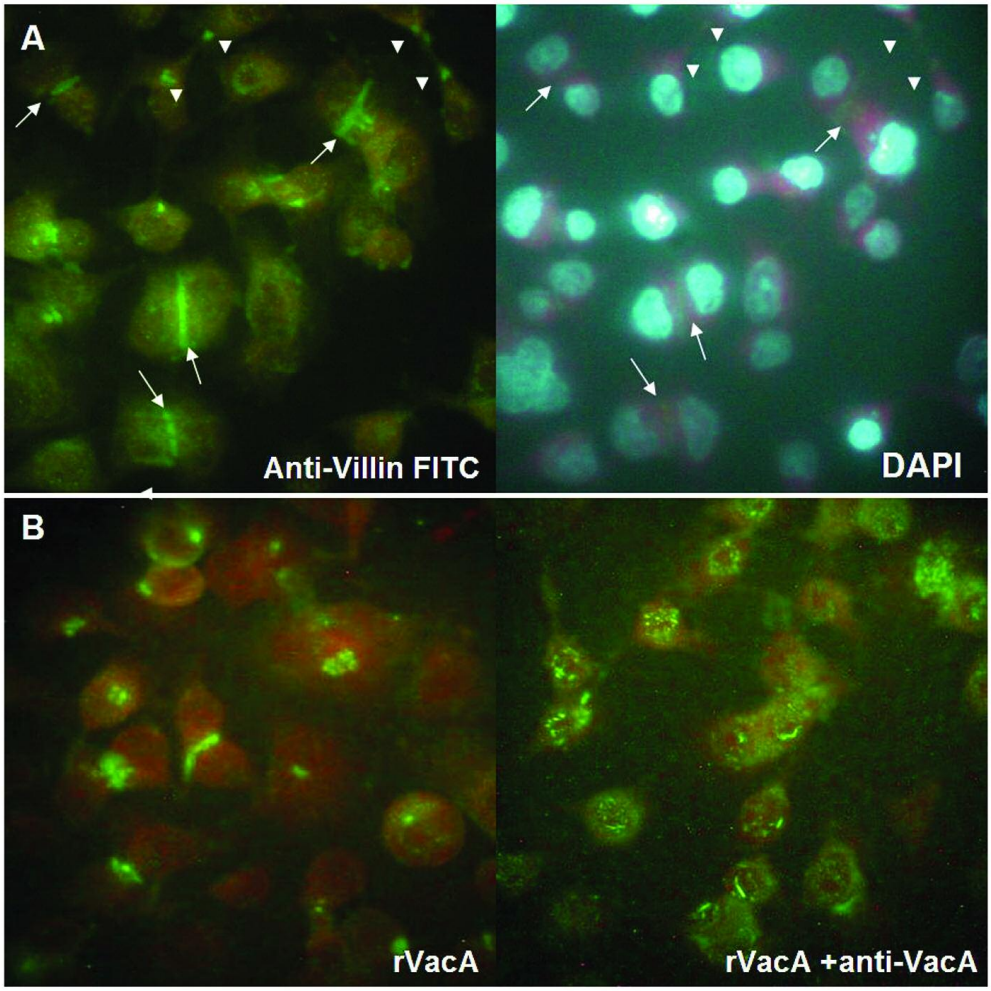

Fig. 12 Immunofluorescent staining for villin in rVacA treated AGS cells.
119x119mm (300 x 300 DPI)